Rapid Molecular Motion of Pyrene and Benzene Moieties Covalently Attached to Silica Surfaces[†]

Michael E. Sigman,[‡] Shelly Read, John T. Barbas, Ilia Ivanov, Edward W. Hagaman,* A. C. Buchanan, III, Reza Dabestani, Michelle K. Kidder, and Phillip F. Britt

Chemical Sciences Division, Oak Ridge National Laboratory, P.O. Box 2008, Oak Ridge, Tennessee 37831

Received: September 11, 2002; In Final Form: December 12, 2002

Remarkably large rotational diffusion rates have been determined for silica-attached 1-pyrene at the solid/air interface through time-dependent fluorescence anisotropy measurements. Diffusion rates $D_{\parallel}$ and $D_{\perp}$ were determined to be 4×10^6 and 2×10^6 s^{-1}, respectively, by treating the motion of the attached moiety as an oblate ellipsoid of rotation. ^{13}C NMR measurements on solid, silica-attached benzene-*1-^{13}C*, acquired using conventional solution NMR methods, gave remarkable, high-resolution spectra. A lower limit for the rate of phenyl group motion was estimated to be 1.5×10^5 s^{-1}, consistent with the fluorescence anisotropy data measured for silica-attached 1-pyrene. Molecular mechanics models for phenyl attached to representative silanol surfaces predict rotational barriers for phenyl rotations in the 2−5 kcal/mol range.

Introduction

The rotational and translational dynamics for molecules confined to surfaces by physical adsorption or chemical attachment play an important role in many chemical reactions and physical processes occurring at interfaces. Our research has been exploring the impact of restricted diffusion on the kinetics and mechanisms of free radical and ionic reactions occurring during the pyrolysis of organic molecules that are covalently immobilized on the surface of nonporous, fumed silica nanoparticles through a thermally robust Si−O−C$_{aryl}$ linkage.[1] The molecules are chosen to mimic related structures present in organic energy resources such as coal and biomass, where restricted diffusion imposed by the cross-linked, macromolecular structure is known to impact thermochemical processing of these materials.[1a]

We have also examined two-component systems in which a probe molecule (e.g., 1,3-diphenylpropane, DPP) was diluted on the surface with spacer molecules either containing benzylic hydrogens (e.g., diphenylmethane) that can be donated to free radical intermediates generated during pyrolysis of the probe molecule or that do not contain donatable hydrogens (e.g., biphenyl).[2] A remarkable 20-fold acceleration in the DPP pyrolysis rate at 375 °C was observed for the diphenylmethane spacer molecule relative to the biphenyl spacer, which is not observed in corresponding fluid-phase studies. The results of detailed kinetic investigations, including isotopic studies with deuterated diphenylmethane, led us to propose a process involving fast serial hydrogen transfer steps on the surface containing the diphenylmethane spacer, which resulted in a radical relay mechanism not involving physical diffusion. This suggested that with hydrogen donor spacer molecules containing more rigid structures, e.g., hydroaromatics such as fluorene, the rate of the bimolecular hydrogen transfer process on the surface could be sensitive to the orientation of the donor molecule. Our preliminary studies of the pyrolysis of DPP in the presence of fluorene spacer molecules attached at either the 2- or 3-positions indicate a ca. 2.3-fold rate increase at 375 °C for the fluorene attached to the surface at the 2-position, indicating that this isomer can attain a more favorable geometry for the critical hydrogen transfer steps.[3]

The research discussed here is of significance in gaining a deeper understanding of the molecular motion of surface-attached aromatic molecules under constrained lateral surface diffusion. Rotational diffusion of the surface-attached moieties constitutes the fundamental process involved in establishing hydrogen atom transfer by a radical relay mechanism on the surface. In the current work, we use silica-attached pyrene and ^{13}C-labeled benzene as probe molecules and time-resolved fluorescence anisotropy, ^{13}C NMR spectroscopy, and molecular modeling to gain new insights into the rotational dynamics of surface-immobilized aromatic moieties.

Materials and Methods

Benzene (Aldrich Chemical Co.) was distilled from sodium prior to use. 1-Hydroxypyrene (Molecular Probes) and phenol-*1-^{13}C* (98 atom % ^{13}C, Icon Services Inc.) were used as received. Fumed silica (Cabosil M-5, Cabot Corp., 200 ± 25 m^2 g^{-1}, N$_2$−BET) was oven dried at 120 °C for 12 h prior to use.

1-Hydroxypyrene or phenol-*1-^{13}C* was chemically attached to the surface of fumed silica by a previously described procedure.[4] Generally, a benzene solution of the 1-hydroxypyrene (hexane:CH$_2$Cl$_2$ 3:1 for phenol-*1-^{13}C*) was slurried with the dry silica at room temperature and the solvent was removed under vacuum to leave a free-flowing solid. The sample was thoroughly degassed (evacuated at 5×10^{-5} Torr) and sealed in a glass ampule prior to the attachment reaction. The attachment reaction was performed by heating the coated silica sample at 225 °C for 1 h in a fluidized sand bath. After surface attachment of the 1-hydroxypyrene or phenol-*1-^{13}C*, the sealed ampule was opened and the silica was washed to remove any phenol that failed to attach. A weighed aliquot of the sample

Motion of Pyrene and Benzene Attached to Silica

J. Phys. Chem. A, Vol. 107, No. 18, 2003 **3451**

was digested in 1 M NaOH, acidified, extracted with CH_2Cl_2, and analyzed by gas chromatography (GC) with an internal standard to determine the surface coverage of the aryl moieties. The recovered phenol was derivatized by silylation with *N,O*-bis(trimethylsilyl)trifluoroacetamide (BSTFA) in pyridine for the GC analysis.

Steady-state fluorescence spectroscopy was performed on solid samples that had been placed in a 1 mm cell, outgassed, and sealed under vacuum. Measurements were conducted on a Spex Fluorolog-2 spectrophotometer equipped with a 450 W Xe lamp and double monochromators on both the excitation and emission sides of the sample compartment. Steady-state fluorescence was collected from the front face of the sample. Steady-state fluorescence polarization measurements were collected using two Glan-Thompson polarizers to adjust the excitation and emission polarization, as previously reported.[5]

Time-resolved anisotropy measurements were conducted by exciting the solid sample with a nitrogen laser (337 nm, 120 μJ per pulse, 4−6 ns pulse width; Laser Science model VSL-337LRF). Excitation was polarized through a Glan-Thompson polarizer prism, and the emission was collected with two lenses and passed through a Glan-Thompson polarizer. Signal collection and digitization is described elsewhere.[5]

Light scattering from the silica surface was shown to have minimal effect on the signal intensity or signal-to-noise ratio of the anisotropy data, and no correction for light scattering was necessary, as previously reported.[5] The time-dependent anisotropy profile was generated from the time-dependent fluorescence according to[6]

$$r(t) = \frac{I_{VV}(t) - G(t)\, I_{VH}(t)}{I_{VV}(t) + 2G(t)\, I_{VH}(t)} \quad (1)$$

In eq 1, $I_{VV}(t)$ and $I_{VH}(t)$ are the time-dependent fluorescence decay profiles observed with the polarization parallel and perpendicular to the direction of the excitation polarization (vertical). The term G is a correction factor required to account for variations in the sensitivity of the detector to vertically and horizontally polarized light. The correction factor G is determined by

$$G(t) = \frac{I_{HV}(t)}{I_{HH}(t)} \quad (2)$$

$I_{HV}(t)$ and $I_{HH}(t)$ are the emission intensities from horizontally polarized excitation monitored with vertical and horizontal polarization, respectively. The denominator of eq 1 represents the total emission.

The anisotropy decay, as calculated from eq 1, was treated theoretically as the anisotropy decay of an oblate ellipsoid of revolution.[6] Oblate ellipsoids (having a unique axis of rotation that is shorter than two other equivalent axes) are expected to display three correlation times (θ_i), as expressed in

$$r(t) = r_1 \exp(-t/\theta_1) + r_2 \exp(t/\theta_2) + r_3 \exp(t/\theta_3) \quad (3)$$

In an oblate ellipsoid, the rate of rotation about the unique axis is designated as $D_{\parallel}$ and the rate of rotation about the other two equivalent axes are designated as $D_{\perp}$. In 1-hydroxypyrene, the unique axis is perpendicular to the plane of the molecule, Figure 1. The absorption (**A**) and emission (**E**) transition moments lie in the plane of the molecule and are perpendicular to the unique axis. Because **A** and **E** lie in the plane of the molecule, the angle between **A** and **E**, β, is equivalent to the angle between the projections of **A** and **E** onto the plane of the molecule, ξ;
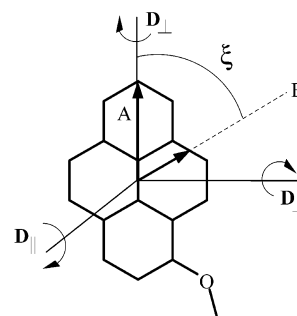

Figure 1. Molecular structure of 1-hydroxypyrene showing rotational diffusion axes and spectroscopic transition moments for oblate ellipsoid treatment.

see Figure 1. The amplitude, r_i, of each component in eq 3 depends on the angles that **A** and **E** make with the unique axis (β_A and β_E, respectively). In the case of 1-hydroxypyrene, β_A and β_E are both 90°, which leads to a simplified double exponential anisotropy decay expression, as given in[6]

$$r(t) = 0.3\cos(2\xi)\exp(-4D_{\parallel}t - 2D_{\perp}t) + 0.1\exp(-6D_{\perp}t) \quad (4)$$

Equation 4 can be fitted to the fluorescence anisotropy decay to obtain values for $D_{\parallel}$, $D_{\perp}$, and ξ, or the correlation times and amplitudes can be determined directly by fitting the anisotropy decay to eq 3. We chose to obtain $D_{\parallel}$, $D_{\perp}$, and ξ from fitting the anisotropy decay to eq 4.

NMR measurements on silica-attached benzene-*1*-^{13}C were performed on a Bruker Avance 400 MHz (9.4 T) NMR spectrometer using standard pulse programs and 5 and 10 mm solution probes. The solid powder was poured into the tube and large voids were removed by compressing the powder with a tamping tool. The sample, restrained using a Teflon vortex plug, was spun along the field axis at 20 Hz and measurements were made in a unlocked mode. Spectra were recorded using single pulse excitation and quadrature detection. Spectra with good signal-to-noise for the ^{13}C-enriched carbon were obtained by signal-averaging 1024 transients. ^{13}C spin−lattice relaxation time (T_1) measurements were made using inversion−recovery (180−t−90) methods and fitting signal intensities measured as a function of t (0−10 s) to

$$I_t = I_0(1 - 2\exp(-t/T_1)) \quad (5)$$

where I_t is magnetization intensity at delay time t following the inversion pulse and I_0 is the intensity of the equilibrium magnetization.

Rotational barriers were calculated by molecular mechanics in HyperChem (Hypercube Inc., V5.0) with the MM+ force field. Two dihedral angles were driven from a modified version of the Microsoft Excel macro provided with the commercial software. The modified macro allowed for the surface-attached moiety and surface silanols to be selected for computational optimization whereas the surface model silicon and oxygen atoms were frozen at their X-ray crystallographic positions.[7] Surface models were based on hydroxylated [111] and [100] planes of β-cristabolite, as detailed in the Results and Discussion.

Results and Discussion

Fluorescence Spectroscopy. The fluorescence spectra of surface-attached 1-pyrene, at a surface coverage of 0.019 and 0.27 mmol/g, are shown in Figure 2. The fluorescence spectrum
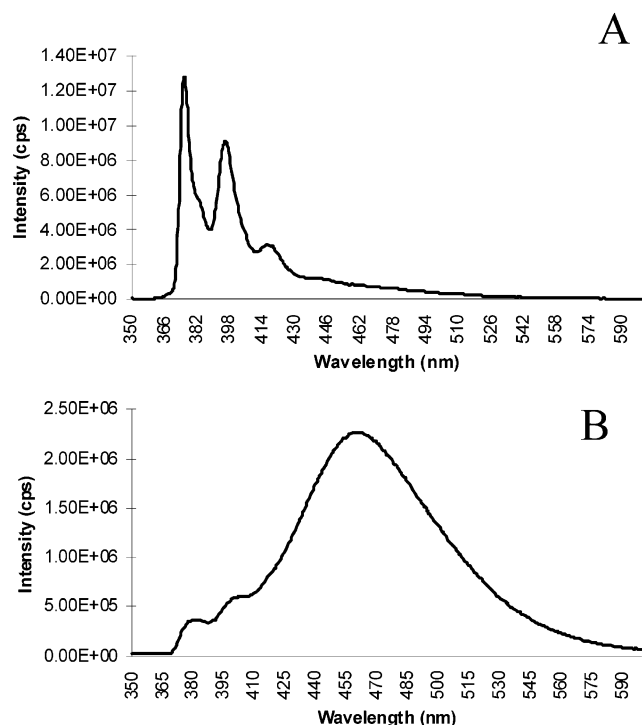
Figure 2. Fluorescence spectra of silica-attached 1-pyrene at surface coverages of (A) 0.019 mmol g^{-1} and (B) 0.2 mmol g^{-1}.

at the lower coverage appears to be almost entirely due to monomer emission, whereas fluorescence at the higher coverage predominantly contains excimer emission. Fluorescence anisotropy measurements were made at the lower coverage to obtain molecular rotational diffusion rates and correlation times for surface-attached monomeric species. Steady-state anisotropy measurements (not shown) on 1-hydroxypyrene in glycerol glass at 77 K gave a fundamental anisotropy of 0.07 ± 0.01 when exciting at 337 nm and monitoring the emission at 397 nm. The 337 nm excitation wavelength corresponds to the wavelength of the nitrogen laser used in the time-resolved studies discussed below. The fundamental anisotropy corresponds to an angle of 48 ± 1° for β, which is equal to ξ as discussed above. The anisotropy measured for surface-attached 1-pyrene (0.019 mmol/g) at room temperature by steady-state spectroscopy (emission at 376 nm) when exciting at 337 nm was 0.03 ± 0.01 ($\beta = 52 ± 1°$).

The room-temperature anisotropy value for the surface-attached sample is lower than the value determined at 77 K due to rotational diffusion effects.[6] The fundamental anisotropy in a rigid system varies with excitation wavelength due to changes in the orientation of the absorption transition moment relative to the emission moment. The anisotropy value is typically independent of the wavelength in the emission spectrum, provided the excitation wavelength is held constant. Invariance of steady-state anisotropy typically observed in an emission spectrum is the result of emission predominantly from the lowest excited state, as described by Kasha's rule.[8] Variation of the steady-state anisotropy observed in an emission spectrum may indicate the presence of multiple emitting species, such as monomer and excimer or impurity. The steady-state anisotropy of the 0.019 mmol g^{-1} surface-attached 1-pyrene observed in the emission spectrum (excitation at 308 nm) was approximately 0.01−0.02 and constant in the 470−500 nm range (not shown). At wavelengths greater than 500 nm, a slight increase in the steady-state anisotropy was observed, and may be attributable to traces of excimer formation. The anisotropy observed in the
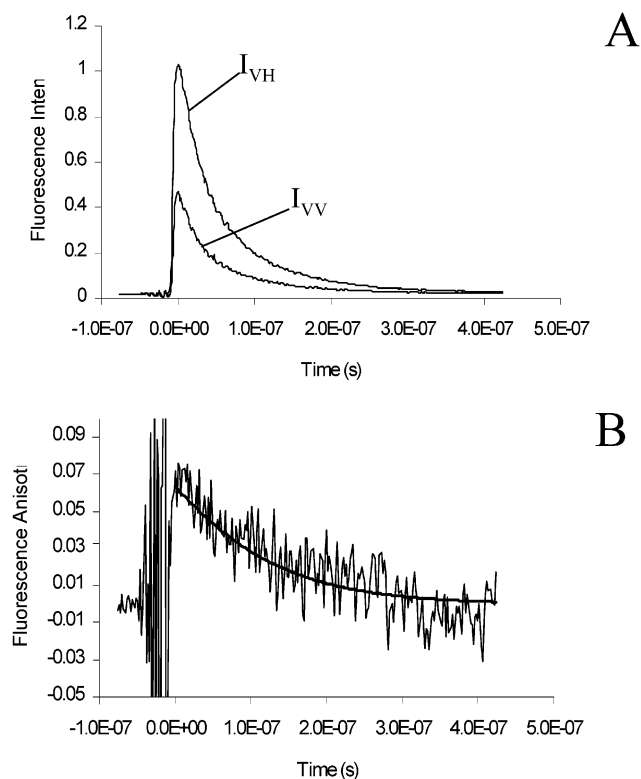

Figure 3. (A) Fluorescence decay curves for silica-attached 1-pyrene at a surface coverage of 0.019 mmol g^{-1}, excitation 337 nm, emission 447 nm. (B) Time-dependent anisotropy calculated from eq 1; see text.

emission spectrum is in good agreement with the value measured in the excitation spectrum at 308 nm (emission monitored at 376 nm).

The time-resolved fluorescence decays measured with vertically polarized excitation and horizontally polarized detection (I_{VH}), and with vertically polarized excitation and vertically polarized emission (I_{VV}), are shown in Figure 3A. The total emission, not shown, is measured with vertical excitation and the emission collected at the magic angle of 54.7°.[6] The time-resolved anisotropy, calculated by eq 1, is shown in Figure 3B with a superimposed decay curve calculated from fitting the experimental data to eq 4. The best-fit values for $D_{||}$ and $D_{\perp}$ were 4×10^6 and 2×10^6 s^{-1}, respectively, with a fitted ξ value of 48°. The rotational correlation times were 40 ns and 80 ns. Although the signal-to-noise ratio is high for the fluorescence decay curves I_{VH} and I_{VV}, the calculated time dependent anisotropy, $r(t)$, contains a higher degree of noise and the fitted values of $D_{||}$, $D_{\perp}$, and ξ are subject to substantial uncertainty. However, the agreement between the fitted value of ξ and the steady-state determination of β lends support to the accuracy of the fitted values. The surprising megahertz rates for $D_{||}$ and $D_{\perp}$ reveal a very rapid motion for the surface-attached aryl moieties. To obtain additional confirmatory evidence of rapid diffusional rates by silica-attached aryl moieties, an investigation of surface-attached benzene-*1*-^{13}C was undertaken.

NMR Spectroscopy. The motion regime in which spin−lattice (T_1) and spin−spin (T_2) relaxation are equal, i.e., the extreme narrowing limit, satisfies the inequality $\omega^2\tau^2 \ll 1$, where ω is the nuclear Larmor frequency and τ is the rotational correlation time. The condition is usually satisfied for molecules in nonviscous solutions where τ is typically 10^{-9} to 10^{-12} rad/s. Although this condition is not satisfied for rotational diffusion rates in the megahertz range, the rates are comparable (order of magnitude) to the ^{13}C Larmor frequency in a 9.4 T magnetic
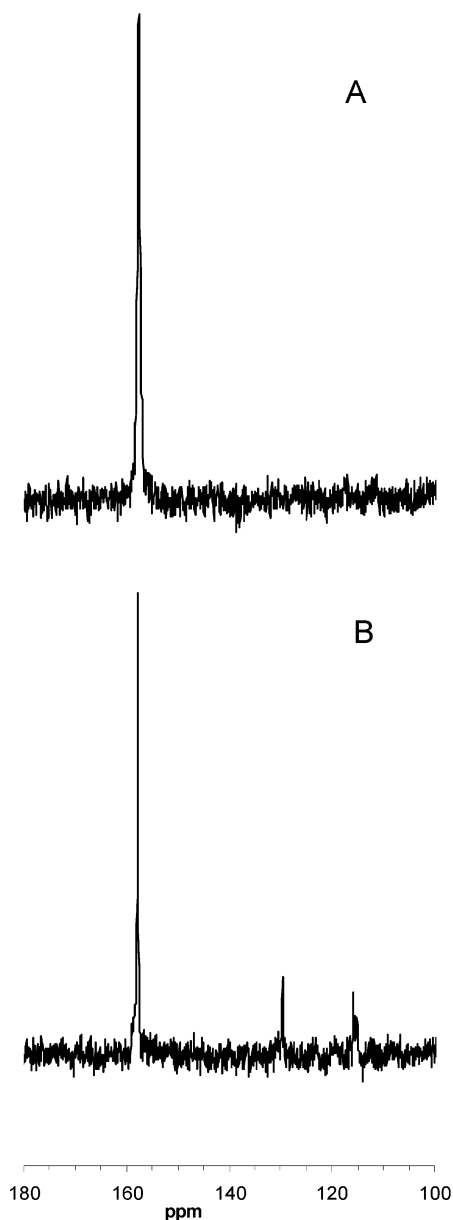
Motion of Pyrene and Benzene Attached to Silica

J. Phys. Chem. A, Vol. 107, No. 18, 2003 **3453**

Figure 4. Single pulse excitation ^{13}C NMR spectra of a powder sample of silica-attached benzene-*1*-[13]*C* recorded in a conventional solution probe spinning along the field axis at 20 Hz: (a) dry powder in a 10 mm sample tube; (b) sample wetted with acetone and recorded in a 5 mm NMR sample tube.

field, 1.0×10^8 Hz, and it may be anticipated that T_1 relaxation is efficient as the phenyl ring rotation rates ascertained from the fluorescence experiments lie near the minimum in the T_1 vs τ curve.[9]

Rotation rates in the megahertz range are sufficient to narrow effectively the phenyl resonances from broadening mechanisms that dominate solid-state spectra, the [13]C−[1]H dipolar and chemical shift anisotropy (CSA) interactions. This reasoning led to recording the ^{13}C NMR spectrum of silica-attached benzene-*1*-[13]*C* (surface coverage = 0.017 mmol g^{−1}) using the normal protocol for a liquid sample.

The spectrum recorded in a 10 mm NMR tube displays a single resonance at 157.8 ppm with half-width of 100 Hz (Figure 4A). The line width decreased to 50 Hz when the spectrum was recorded in a 5 mm NMR tube. Thus a major fraction of the broadening is due to field inhomogeneity. The line width of the resonance further decreased when the solid was wetted with

acetone. The line width became 13 Hz, increasing the signal-to-noise enough that the protonated ring carbons at natural abundance ^{13}C levels become evident in the spectrum (129.3 ppm, meta; 115.4 ppm, ortho; 115.2 ppm, para; Figure 4B). This suggests a magnetic susceptibility broadening mechanism is responsible for a fraction of the line width.[10] It is also possible that the solvent molecules envelop the surface-attached benzene moieties, creating a more uniform local environment. In any event, the liquidlike resonance seen in Figure 4 is clear evidence of rapid rotational motion of the phenyl group in silica-attached benzene-*1*-[13]*C*.

The spin−lattice relaxation time of C(1) of the silica-attached benzene-*1*-[13]*C* is 2.0 ± 0.2 s. It is well-known that spin−lattice relaxation time and nuclear Overhauser enhancement (NOE) measurements allow the [13]C−[1]H dipolar contribution to the spin−lattice relaxation rate to be separated from all other contributing mechanisms.[11] Protonated carbons in organic molecules relax predominantly by a [13]C−[1]H dipolar mechanism whereas nonprotonated aromatic carbons relax mostly through chemical shift anisotropy (CSA) in measurements made at 7 T.[12] CSA is the only relaxation mechanism that is field dependent and can be expected to dominate relaxation rates of nonprotonated aromatic carbons in measurements made at 9.4 T. This is shown by measurement of the NOE observed for the enriched carbon of the silica-attached benzene-*1*-[13]*C*: NOE = $1 + \eta = 1 + 0.21 = 1.21$, where η is the incremental increase in resonance intensity measured in proton decoupled ^{13}C NMR spectra relative to the signal in coupled or gated noise-decouple spectra. From η and T_1 it follows that 10% of the relaxation rate is due to [13]C−[1]H dipolar relaxation; the dominant relaxation mechanism, accounting for 90% of the rate, is CSA.[12]

The rigid lattice line width of the C(1) resonance will be dominated by the CSA contribution. The anisotropy of phenolic carbon is 150 ppm, or 15 kHz at 9.4 T.[13] Roughly, it is with respect to this frequency that motion must be rapid if a narrow resonance is observed. Thus, a lower limit estimate for the rotational rate of the phenyl group is 1.5×10^5 s^{−1}, in good agreement with the estimates from fluorescence spectroscopy.

Molecular Models. Molecular models of the silica surface were developed to aid in realistic visualization of the rotational diffusion process for surface-attached aryl moieties and to provide approximate energy barriers for rotational diffusion. Silica surfaces can be visualized as being composed of a set of domains corresponding to the hydroxylated [100] and [111] crystallographic planes of β-cristobalite.[14] The hydroxylated [100] plane contains only geminal (designated Q2) silanols at a number density of 7.88 hydroxyls per nm[2]. The hydroxylated [111] plane contains only isolated (Q3) silanols at a number density of 4.55 hydroxyls per nm[2]. Large models of silica surfaces can be constructed from intersecting hydroxylated [111] and [100] faces of β-cristobalite.[14] The surface of Cabosil fumed silica used in this work has been determined by ^{29}Si NMR studies to be composed of 64.5% isolated, Q3, silanols. The remaining silanols are of the geminal, Q2, form. The average number density of hydroxyls for this mixed surface is 5.7 hydroxyls per nm[2], corresponding to 1.9 mmol of hydroxyls per gram of silica (based on a N_2−BET surface area of 200 m[2] g^{−1}). The 1-pyrene surface loading of 0.019 mmol g^{−1} corresponds to an average of 1% derivatization of surface silanols. The benzene-*1*-[13]*C* coverage, 0.017 mmol g^{−1}, similarly occupies close to 1% of the surface silanols.

Small molecular models of hydroxylated [111] and [100] planes of β cristobalite are shown in Figure 5, along with
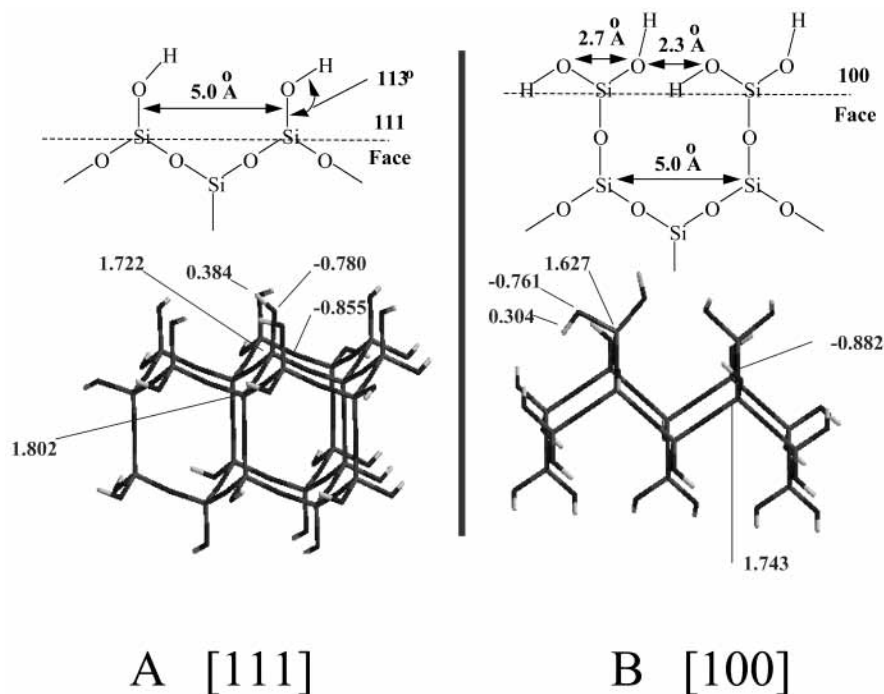
Figure 5. Molecular models of hydroxylated (A) Si [111] and (B) [100] surfaces, relevant distances and atomic charges (MNDO/d).
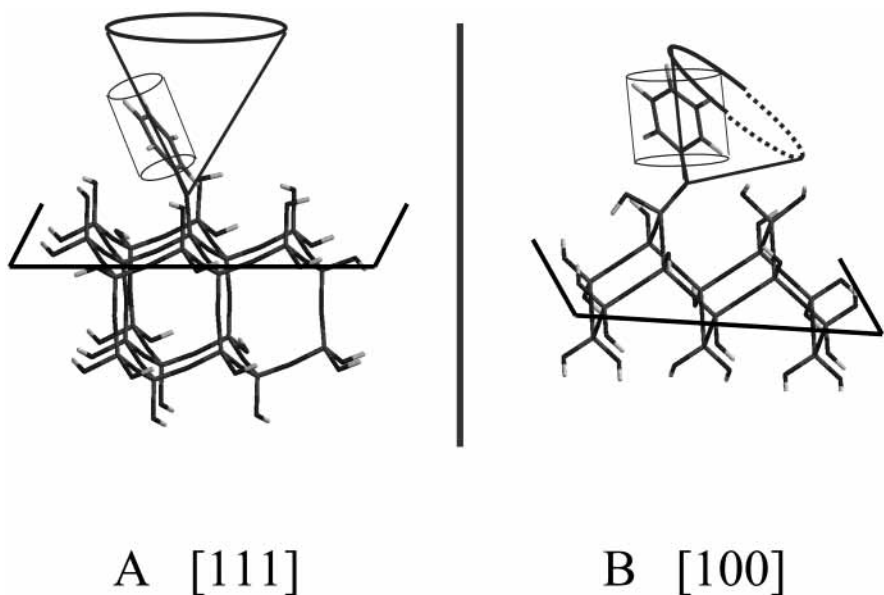

Figure 6. Molecular models of hydroxylated (A) Si[111] and (B) [100] surfaces with covalently attached phenyl moieties.

important bond distances, angles and calculated (MNDO/d) charges. The positions for the Si and O atoms in the models correspond to X-ray crystallographic data.[7] Figure 6 depicts models of surface-attached phenyl moieties and the cones (O—Si—O—C dihedral designated ϕ) and cylinders (Si—O—C=C dihedral designated ψ) of rotation accessible to attached phenyls on [111] and [100] surfaces. Phenyl moieties attached to a [111] surface model can experience full rotation about both ψ and ϕ dihedral angles, whereas on the [100] surface model, rotation about ϕ is restricted by the neighboring geminal silanols on the surface; see Figure 6.

The energy barriers to rotation about both ψ and ϕ dihedrals were calculated for a phenyl attached to each surface model using the molecular mechanics (MM+ force field) method. The MM+ force field is based on MM2 force field, which is known to give conformational energies with errors of approximately

0.5 kcal/mol.[15] Figure 7 shows the calculated energy surfaces for each model.

In the [100] model, a minimum on the ϕ–ψ mapped energy surface occurs at an O—Si—O—C dihedral (ϕ defined as shown by the dashed line in Figure 7A) angle of 60°. Rotation of the Si—O—C=C dihedral (ψ) encounters a modest barrier of 4.5 kcal mol^{-1} at ϕ near its minimum. However, the energy rapidly climbs to values exceeding 10 kcal mol^{-1} above the minimum as ϕ is increased to 100–150°. The rapid increase is due to steric interaction between the phenyl moiety and the adjacent geminal silanols and lattice constituents (Si and O). The resulting picture is one of the surface-attached phenyl moving between two minima along dihedral ϕ, separated by a barrier at 0°, imposed by eclipsing the O—Si and O—C bonds.

In the [111] surface model, the lowest barrier (ca. 2 kcal mol^{-1}) for rotation about the Si—O—C=O dihedral (ψ) occurs
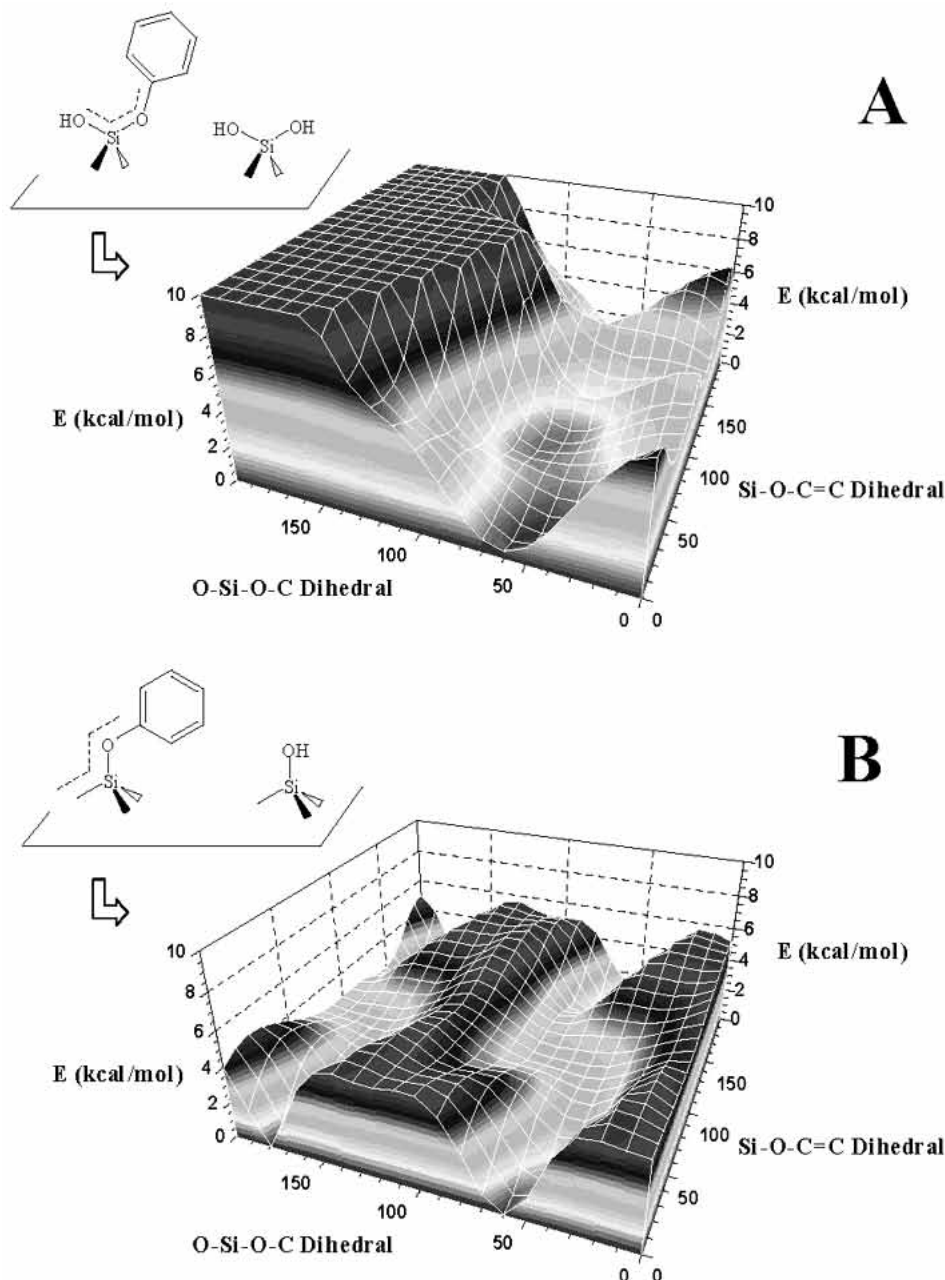
Figure 7. Energy surfaces for O—Si—O—C and Si—O—C=C dihedral angles calculated by molecular mechanics (MM+) for the models shown in Figure 6: (A) phenyl attached to Si [100] model and (B) phenyl attached to Si [111].

at an O—Si—O—C dihedral angle (ϕ) of 60°, as defined in Figure 7B. Unlike the [100] case, rotation about ϕ encounters a modest barrier of 4.3 kcal/mol at $\psi = 90°$, and the barrier imposed by steric interactions with the [100] surface are absent. The $\phi-\psi$ mapped energy surface for the [111] silica model has an anticipated 3-fold barrier for rotation about ϕ that is imposed by the tetrahedral bonding around Si, with additional features imposed by interactions of the phenyl moiety with neighboring Q3 silanols. The minimum energy along ϕ corresponds to the three gauche orientations. Rotation of the phenyl moiety about the ψ dihedral is accompanied by correlated motion in ϕ, as shown in Figure 7B.

The calculated energy barriers shown in Figure 7 suggest that diffusional motion of surface-attached moieties is favored through rotation about ψ. The calculated barriers are low and support the experimental observations of megahertz rotational diffusion rates for surface-attached aryl moieties on silica surfaces.

Conclusions

We have demonstrated that aryl moieties attached to silica surfaces through silanol ether (Si—O—C$_{Ar}$) linkages undergo megahertz rotational diffusion at ambient temperatures. Time-dependent fluorescence anisotropy, ^{13}C NMR and molecular modeling data provide compelling evidence for this surprising result. The most significant ramification of these findings may be the ability to conduct NMR studies on isotopically enriched samples using a standard liquid sample protocol.

References and Notes

(1) (a) Buchanan, A. C., III; Britt, P. F. *J. Anal. Appl. Pyrol.* **2000**, *54*, 129−153. (b) Buchanan, A. C., III; Britt, P. F.; Skeen, J. T.; Struss, J. A.; Elam, C. L. *J. Org. Chem.* **1998**, *63*, 9895−9903. (c) Britt, P. F.; Buchanan, A. C., III; Malcolm, E. A. *Energy Fuels* **2000**, *14*, 1314−1322.

(2) Buchanan, A. C., III; Britt, P. F.; Thomas, K. B.; Biggs, C. A. *J. Am. Chem. Soc.* **1996**, *118*, 2182−2189.

(3) Buchanan, A. C., III. Unpublished data.

(4) Buchanan, A. C., III; Dunstan, T. D. J.; Douglas, E. C.; Poutsma, M. L. *J. Am. Chem. Soc.* **1986**, *108*, 7703.

(5) Ivanov, I. N.; Dabestani, R.; Buchanan, A. C., III; Sigman, M. E., *J. Phys. Chem. B* **2001**, *105*, 10308.

(6) Lackowicz, J. R. *Principles of Fluorescence Spectroscopy* 2nd ed.; Kluwer Academic/Plenum Publishers: New York, 1999.

(7) Wright, A. F.; Leadbetter, A. J. *Philos. Mag.* **1975**, *31*, 1391.

(8) Kasha, M. *Discuss. Faraday Soc.* **1950**, *9*, 14.

(9) Pople, J. A.; Schneider, W. G.; Bernstein, H. J. *High-resolution Nuclear Magnetic Resonance*; McGraw-Hill Book Co.: New York, 1959; p 205.

(10) VanderHart, D. L.; Earl, W. L.; Garroway, A. N. *J. Magn. Reson.* **1981**, *44*, 361−401.

(11) Lyerla, J. R., Jr.; Grant, D. M.; Harris, R. K., *J. Phys. Chem.* **1971**, *75*, 585−588.

(12) Alger, T. D.; Hamill, W.D., Jr.; Pugmire, R. J.; Grant, D. M.; Silcox, G. D.; Solum, M. *J. Phys. Chem.* **1980**, *84*, 632−636. Alger, T. D.; Solum, M.; Grant, D. M.; Silcox, G. D.; Pugmire, R. J. *Anal. Chem.* **1981**, *53*, 2299−2304.

(13) Orendt, A. M.; Solum, M. S.; Sethi, N. K.; Craig, D. H.; Pugmire, R. J.; Grant, D. M. *Measurement of ^{13}C Chemical Shift Anisotropies in Coal*; In Magnetic Resonance of Carbonaceous Solids; Botto, R. E., Sanada, Y., Eds.; Advances in Chemistry Series 229; American Chemical Society: Washington, DC, 1993.

(14) (a) Liu, C. C.; Maciel, G. E. *J. Am. Chem. Soc.* **1996**, *118*, 5103. (b) Chuang, I. S.; Maciel, G. E. *J. Phys. Chem. B* **1997**, *101*, 3052.

(15) Gundertofte, K.; Liljefors, T.; Norrby, P.; Pettersson, I. *J. Comput. Chem.* **1996**, *17(4)*, 429.